# Effect of impurities on incommensurate spin fluctuations in a *d*-wave superconductor

De-Cai Zhang and Jian-Xin Li
*Department of Physics and National Laboratory of Solid State Microstructures, Nanjing University, Nanjing 210093, China*
(Received 8 June 2009; published 25 November 2009)

The effects of nonmagnetic impurity on the spin response in a $d_{x^2-y^2}$-wave superconductor are studied theoretically. Starting from the dispersion derived from the mean-field $t$-$t'$-$J$ model, we carry out the calculations based on the self-consistent $t$-matrix approximation and the random phase approximation. The effect of impurity is treated both via the self-energy correction and the vertex correction. It is found that the incommensurate (IC) spin fluctuations at frequencies above the spin gap are enhanced notably and the incommensurability is reduced, when impurities are introduced. These effects are less prominent with the increase in dopings. For low frequencies in the spin gap the IC spin fluctuations is enhanced with no reduction in incommensurability. The vertex corrections within the ladder approximation do not significantly modify the renormalized-bubble result, but it induces additional excitations in the spin gap. These results are qualitatively consistent with experiments.

DOI: 10.1103/PhysRevB.80.174523 PACS number(s): 74.25.Ha, 74.20.Mn

## I. INTRODUCTION

Neutron scattering has revealed rich characteristics of the spin fluctuations in the hole-doped high-$T_c$ cuprates.[1] At low frequencies, the spin fluctuations show the incommensurate (IC) peaks at the wave vectors $(\pi, \pi \pm x\pi)$ and $(\pi \pm x\pi, \pi)$. The incommensurability $x$ decreases with the increase in frequency, so the spin excitations exhibit a downward dispersion.[2–4] At the antiferromagnetic (AF) wave vector $(\pi, \pi)$, the so-called spin resonance mode appears, which manifests as a resolution-limited resonance peak in the frequency dependence of the spin fluctuations.[2,3,5] When frequency is above the spin resonance, the incommensurability reemerges and increases with frequency, therefore shows an upward dispersion.[6–8] Thus, the spin fluctuation in the hole-doped cuprates shows a universal hourglass-like dispersion.

Theoretically, the possible explanations for the nature of spin excitations in the hole-doped cuprates may be roughly divided into two groups. One is the weak-coupling Fermi-liquid theory based on the topology of underline Fermi surface.[9–12] In this picture, the incommensurate spin fluctuations come from the nesting of the Fermi surface[11,12] and the spin resonance is ascribed to a spin collective mode (spin exciton).[9–11] The other is based on the stripe scenario in which the doped holes are arranged in one-dimensional lines and form the so-called charge stripe separating the AF domains.[13] Due to the modulation of the charge stripes (they act as antiphase domain walls for the AF order), the magnetic excitations exhibit the incommensurate structure. The resonance excitations is associated with the accumulation of the spectral weight around the AF wave vector.[14,15] Basically, the former approach emphasize on the charge degree of freedom, while the latter has the advantage of treating the quantum-mechanical nature of the spins.

In the study of high-$T_c$ cuprates, impurity substitution for planar Cu sites can be chosen so as to affect its physical properties, such as the magnetic excitations. In this regard, zinc is a usually used nonmagnetic impurity element, since it has almost the same atomic mass as copper but a different spin state. The substitution of nonmagnetic impurities for Cu atoms changes the magnetic environment near the impurity atoms and gives rise to some modifications of spin[16–19] and electronic properties.[21–23] For example, the smearing out of the spin resonance[16,18] and of the peak/dip/hump structure in the electronic lineshape[20,21] by the zinc doping have been found. Recently, it is observed that zinc substitution in the Cu-O plane of $La_{2-x}Sr_xCuO_4$ (LSCO) gives birth to a smaller incommensurability and induces an anomalous enhancement of the low-energy scattering spectra around the AF wave vector,[24,25] forming a flat-top structure for spin fluctuations. For system with lower hole doping, the effect of the incommensurability reduction and the peak enhancement is more prominent than the system with higher hole doping.[24] Meanwhile, the "spin gap" which exists in the impurity-free samples vanishes as the impurity concentration is increasing, which is probably caused by the emergency of the in-gap states.[16,25]

Motivated by the above experimental facts, in this paper we will investigate the effect of nonmagnetic impurity on the incommensurate spin fluctuations in a $d_{x^2-y^2}$-wave superconductor. Our study is based on the weak-coupling Fermi-liquid approach, so it is not our intent to compare the two approaches mentioned above. Instead, we wish to know if the nonmagnetic impurity effect on the spin excitations can be reasonable accounted for by the weak-coupling approach. Impurities are considered in the dilute limit and their effects are treated using the self-consistent $t$-matrix approximation. Our calculation is carried out first based on the self-energy correction caused by the impurity. We find that, with the introduction of impurities, the IC peaks along the $(\pi \pm \delta, \pi)$ and its symmetric directions in the low-energy region above the spin gap are enhanced, and the incommensurability are reduced. While inside the spin gap, the IC peaks and the whole lineshape are enhanced notably with no reduction in incommensurability. For the system with a higher hole doping level, the impurity effects are less prominent. Furthermore, we include the contribution of vertex corrections within the ladder approximation, and find that it introduces additional excitations in the spin gap region, but does not significantly modify the renormalized-bubble result. These

 

results are qualitatively consistent with experiments.

The article is organized as follows. In Sec. II, we introduce the model, and present the results with the inclusion of the impurity self-energy correction. In Sec. III, we consider the effect of the impurity vertex correction. In Sec. IV, we give our conclusion.

## II. SELF-ENERGY CORRECTION

We start with the following mean-field Hamiltonian of a $d$-wave superconductor[26]

$$H_m = \sum_{k\sigma} \xi_k f^+_{k\sigma} f_{k\sigma} - \sum_k \Delta_k (f^+_{k\uparrow} f^+_{-k\downarrow} + \text{c.c.}) + \xi_0, \tag{1}$$

with $\xi_k = -2(\delta t + J'\chi_0)(\cos k_x + \cos k_y) - 4\delta t' \cos k_x \cos k_y - \mu$, $\Delta_k = 2J'\Delta_0(\cos k_x - \cos k_y)$, and $\xi_0 = 2NJ'(\chi_0^2 + \Delta_0^2)$. This dispersion can be derived from the slave-boson mean-field calculation of the $t$-$t'$-$J$ model,[11,26] here we take it as a phenomenological form. In the dispersion relationship, $\delta$ is the doping level. $t(t')$ is the nearest (next-nearest) hopping integral. $\chi_0$ and $\Delta_0$ are mean-field parameters. $J' = 3J/8$ which arises from the decoupling of the AF Heisenberg term ($J$ term in the $t$-$t'$-$J$ model) into three different channels.[26] The reason we choose this form is that in this way the parameters $\chi_0$, $\Delta_0$ and the chemical potential $\mu$ can be determined self-consistently for a given doping level $\delta$. This allows us to carry out a systematic doping-dependent investigation. By minimizing the free-energy $F = -\frac{1}{\beta}\ln \text{Tr}(e^{-\beta H_m})$, one can get the self-consistent equations,

$$\chi_0 = -\frac{1}{2N}\sum_k \tanh\left(\frac{1}{2}\beta E_k\right)\frac{\xi_k \gamma_k}{E_k}, \tag{2}$$

$$1 = \frac{1}{N}\sum_k \tanh\left(\frac{1}{2}\beta E_k\right)\frac{J'\phi_k^2}{E_k}, \tag{3}$$

$$\delta = \frac{1}{N}\sum_k \tanh\left(\frac{1}{2}\beta E_k\right)\frac{\xi_k}{E_k}, \tag{4}$$

with $\gamma_k = \cos k_x + \cos k_y$, $\phi_k = \cos k_x - \cos k_y$, and $E_k = \sqrt{\xi_k^2 + \Delta_k^2}$. In the following, $t = 2J$ and $t' = -0.45t$ are chosen.

Considering impurity effects, we have the impurity-averaged Green's function for single particle in the Nambu representation,[27–29]

$$\hat{G}(\mathbf{k}, i\omega_n) = \frac{i\tilde{\omega}_n \hat{\sigma}_0 + \tilde{\Delta}_k \hat{\sigma}_1 + \tilde{\xi}_k \hat{\sigma}_3}{(i\tilde{\omega}_n)^2 - \tilde{\Delta}_k^2 - (\tilde{\xi}_k)^2}, \tag{5}$$

where $\hat{\sigma}_m (\hat{\sigma}_0 = \hat{\mathbf{1}})$ is the Pauli matrix. The tilde symbol indicates the inclusion of impurity-scattering self-energy corrections, which is introduced via the Dyson equation $\hat{G}^{-1} = \hat{G}_0^{-1} - \hat{\Sigma}$ with $\hat{G}_0^{-1}$ the impurity-free Green's function and the self-energy having components,

$$\tilde{\omega}_n = \omega_n - \Sigma_0(\omega_n), \tag{6}$$

$$\tilde{\Delta}_k = \Delta_k + \Sigma_1(\omega_n), \tag{7}$$

$$\tilde{\xi}_k = \xi_k + \Sigma_3(\omega_n). \tag{8}$$

For a $d$-wave superconducting (SC) gap, the correction to the gap function $\Sigma_1$ vanishes.[27] In dilute limit, we can neglect the interactions between impurities and take the single-site approximation. Then the impurity self-energy will be given by $\Sigma_j = \Gamma_0 T_j$. The impurity-scattering $t$-matrix $T_j$ can be calculated from,[27]

$$T_0 = \frac{G_0(\omega)}{c^2 - [G_0(\omega)]^2}, \quad T_3 = \frac{-c}{c^2 - [G_0(\omega)]^2}, \tag{9}$$

with $G_0(\omega) = (1/\pi N_0)\Sigma_k \text{Tr}[\hat{\sigma}_0 \hat{G}(\mathbf{k}, \omega)]$. Here, $c = \cot \delta_0$ and $\Gamma_0 = n_i/\pi N_0$. $N_0$ is the normal phase density of states, $n_i$ the impurity concentration, and $\delta_0$ the scattering phase shift. Because the zinc impurity has a strong effect on the SC properties, it is generally treated in the unitary limit,[30] i.e., $c = 0$. So only $\Sigma_0$'s contribution remains. In the presence of impurities, the superconducting energy gap $\Delta(\Gamma_0, 0)$ and the transition temperature $T_c$ need to be determined from the gap equation. Nonmagnetic impurities are pair breakers in the anisotropic superconductors such as high-$T_c$ cuprates.[30,33] Hence, in the weak-coupling limit we have the relationship: $\Delta(\Gamma_0, 0)/\Delta_0 \approx T_c/T_{c0}$,[31] with $T_{c0}$ the transition temperature in the impurity-free system. The temperature-dependent energy gap $\Delta(\Gamma_0, T)$ is

$$\Delta(\Gamma_0, T) = \Delta(\Gamma_0, 0)\tanh[2\sqrt{(T_c/T) - 1}], \tag{10}$$

where $T_c$ is given by the generalization of the Abrikosov-Gor'kov formula[32] to the anisotropic superconductors as shown in Ref. 33,

$$-\ln\left(\frac{T_c}{T_{c0}}\right) = \psi\left(\frac{1}{2} + \frac{\Gamma_0}{2\pi T_c}\right) - \psi\left(\frac{1}{2}\right), \tag{11}$$

with $\psi(x)$ the digamma function.

With the impurity-averaged Green's function, the spin susceptibility can be obtained from the following response function in Matsubara frequency by an analytical continuation to the real frequency $\chi_0(i\omega_m \to \omega + i0^+)$,

$$\chi_0(\mathbf{q}, i\omega_m) = -\frac{T}{N}\sum_n \sum_k \text{Tr}\left[\frac{1}{2}\hat{G}(\mathbf{k}, i\omega_n)\cdot \hat{G}(\mathbf{k}+\mathbf{q}, i\omega_m + i\omega_n)\right]. \tag{12}$$

The analytical continuation is performed numerically by using the Padé approximants.[34]

To consider the correction from spin fluctuations, we should go beyond the mean-field level [expressed by Eq. (1)] to include the interaction between fermions. This amounts to add an interaction term $H_I$ to Eq. (1), i.e., $H = H_m + H_I$ with $H_I = U\Sigma_i f^\dagger_{i\uparrow} f_{i\uparrow} f^\dagger_{i\downarrow} f_{i\downarrow}$ [$i$ denotes the lattice site]. For the spin fluctuation, the usual random phase approximation (RPA) selects a series of bubble diagrams and results in the renormalized spin susceptibility as given by,[9–12,35]

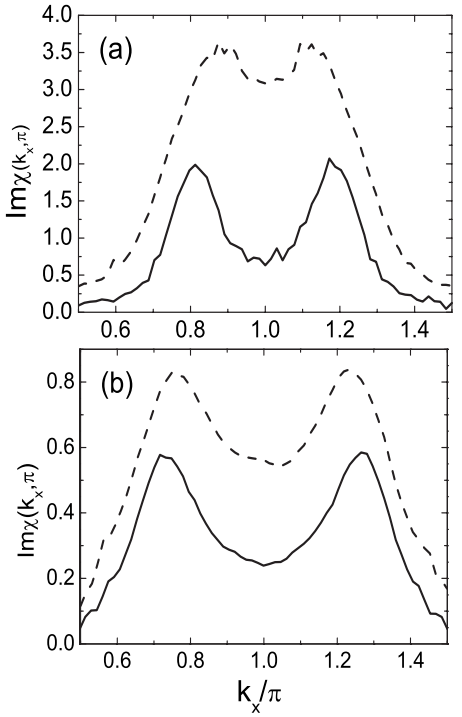


FIG. 1. Im $\chi$ versus $k_x(k_y=\pi)$ for the pristine system (solid line) and that with impurity concentration $\Gamma_0/\Delta_0=0.04$ (dashed line) at $\omega=0.2J$ above the spin gap. (a) is for doping $\delta=0.1$ and (b) for doping $\delta=0.15$.

$$\chi(\mathbf{q},\omega)=\frac{\chi_0(\mathbf{q},\omega)}{1-U\chi_0(\mathbf{q},\omega)}. \tag{13}$$

The criteria for choosing the value of $U$ is to set the spin resonance peak of the pristine system at the experimental value.[1] This gives $U=0.9$, which corresponds to the resonance peak at $0.375J\approx 45$ meV (taking $J=120$ meV).

Though a hourglass dispersion of spin excitations has been observed by neutron scattering,[6–8] the weak-coupling approach adopted here is applicable basically to the description of spin excitations below the spin resonance where the particle-hole excitations contributing to the spin susceptibility are well defined.[11,12] Below the spin resonance $0.375J$, the spin susceptibility Im $\chi$ shows an incommensurate structure in the momentum space with the IC peaks at $(\pi\pm x\pi,\pi)$ and its symmetric directions. Around the IC peak, we find that the spin gap is about $0.09J$ in the pristine system. The spin gap is decreased when increasing the impurity concentration, for example it is $0.08J$ for impurity concentration $\Gamma_0/\Delta_0=0.04$ and $0.06J$ for 0.08. We will first discuss the result at low frequencies above the spin gap. Typically, Fig. 1 shows Im $\chi$ versus $k_x(k_y=\pi)$ at frequency $\omega=0.2J$, with the hole doping level $\delta=0.1$ [Fig. 1(a), underdoped] and $\delta=0.15$ [Fig. 1(b),optimally doped]. The solid line is for the pristine system, and the dashed line is for the system with a impurity concentration $\Gamma_0/\Delta_0=0.04$. For the pristine system, the lineshape shows two IC peaks, with the incommensurability $x=0.18$. When impurities are introduced, the lineshape is modified in two ways. First, as a whole the intensity of Im $\chi$ is enhanced noticeably. The enhancement in intensity occurs more remarkably near the $(\pi,\pi)$ point and at the meantime the IC peaks are broadened. As a result, the modified lineshape exhibits a weaker IC-peak structure, forming a flat-top shape. This is consistent with experiments.[24] Another interesting feature is the reduction in the incommensurability. For the impurity-doped system, the incommensurability is $x=0.12$. So, the reduction in the incommensurability is 0.06. With the increase in hole doping level, such as for $\delta=0.15$ as shown in Fig. 1(b), one sees that the enhancement in Im $\chi$ is relatively smaller than that in the underdoped system with $\delta=0.1$. Moreover, due to the fact that the anisotropy in the enhancement is relatively smaller, so the IC-peak structure still remains. In this case, the reduction in the incommensurability is found to be $0.05\pi$, which is also smaller than that in the underdoped system. The doping dependence of the incommensurability for the systems without and with impurity is shown in Fig. 2. One can see that the reduction in the incommensurability decreases with the increase in dopings. These two main features: (i) an overall enhancement of Im $\chi$ occurs with the inclusion of the impurity scattering, and the enhancement becomes less effective with the increase in hole doping, (ii) the incommensurability is reduced by impurities, and the reduction becomes smaller with the increase in hole doping, are consistent with the experimental facts.[24]

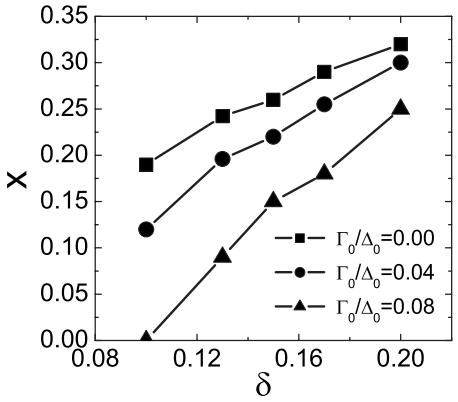


FIG. 2. Doping dependence of the incommensurability $x$ in the $(\pi\pm x\pi,\pi)$ direction for the pristine system (squares) and that with impurity concentration $\Gamma_0/\Delta_0=0.04$ (circles) and $\Gamma_0/\Delta_0=0.08$ (triangles). The frequency is at $\omega=0.2J$.

In the scenario of Fermi-liquid type theory, the incommensurate spin fluctuation is interpreted by the nesting effect of the Fermi surface.[11,12] In an SC state, the spin susceptibility arises from the scattering of the SC quasiparticles across the SC gap. Hence, the nesting involves an equal energy contour determined by $(\omega-\mathrm{Re}\,\Sigma_0)/2=(\xi_k^2+\Delta_k^2)^{1/2}$ In Fig. 3, we present the equal energy contour for $\omega=0.2J$ which is the same frequency as used for getting the results in Fig. 1. The arrows indicate the best nesting vectors connecting the two flat pieces of the energy contour. An obvious difference between the pristine and the impurity-doped systems is that the nesting portion of the contour connected by the nesting vector is enlarged upon the introduction of impurity and this effect is less effective as hole doping is increased. As a result, it will lead to an enhancement of the IC-peak intensity and the enhancement decreases with the increase in hole doping, as shown in Fig. 1.

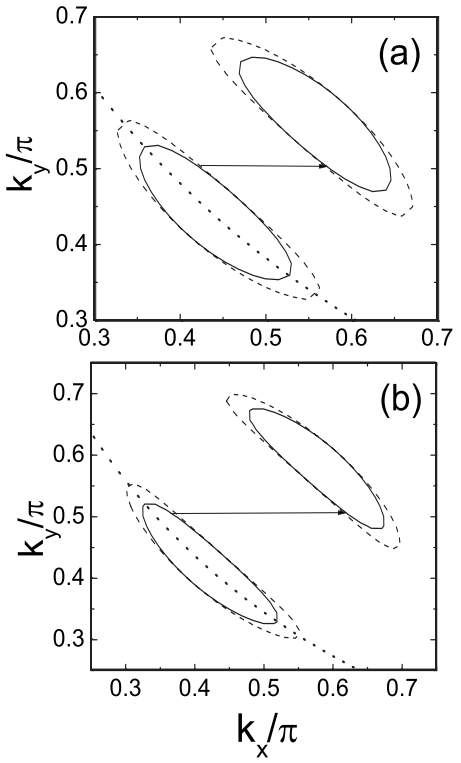


FIG. 3. Equal energy contours of the SC quasiparticle energy $E_k$ at $E_k=\omega/2=0.1J$ for the hole doping (a) $\delta=0.1$ and (b) $\delta=0.15$. The solid line is for the impurity concentration $\Gamma_0/\Delta_0=0$ and the dashed line for $\Gamma_0/\Delta_0=0.04$. The arrows indicate the best nesting vectors and the dotted lines the normal state Fermi surface in the impurity-free system.

In Fig. 4, we present the contour plots of the velocity of the SC quasiparticles ($v_{k_i'}=dE_{k'}/dk_i'$, $E_{k'}$ the SC quasiparticle energy) in the coordinate system $(k_x',k_y')$ which is rotated $\pi/4$ with respect to the original coordinates $(k_x,k_y)$ [see Fig. 4(c)]. We find that the $x'$ direction component $v_{k_x'}$ of the velocity has less change upon the introduction of impurity, as shown in Fig. 4(a1) and Fig. 4(a2). While, the $y'$ direction component $v_{k_y'}$ decreases noticeable when the effect of impurity is included [see Fig. 4(b1) and Fig. 4(b2)]. This difference comes from the effect that the SC gap magnitude decreases due to the impurity as can be inferred from Eqs. (10) and (11). For a $d_{x^2-y^2}$ gap symmetry, the SC gap has a vanishing value around the diagonal direction, while it becomes larger when moves away from the diagonal direction along the Fermi surface. So, the reduction in the SC gap magnitude upon impurity-doping will be much more effective near the end of the equal energy contour along the $k_y'$ direction. This explains the results presented in Fig. 4, in which the equal energy contour extends along the $k_y'$ direction when impurities are introduced. On the other hand, the effect of impurity also enters via the self-energy $\Sigma_0$. The frequency dependence of $\Sigma_0$ is presented in Fig. 5. Though its real part exhibits a peak around $0.12J$ [Fig. 5(a)], the magnitude is too small to have an obvious effect on the equal energy contour. In correspondence with this peak, its imaginary part $-\mathrm{Im}\,\Sigma_0$ shows a step-like increase at low frequencies,[36] consequently it broadens the IC-peak width as shown in Fig. 1.

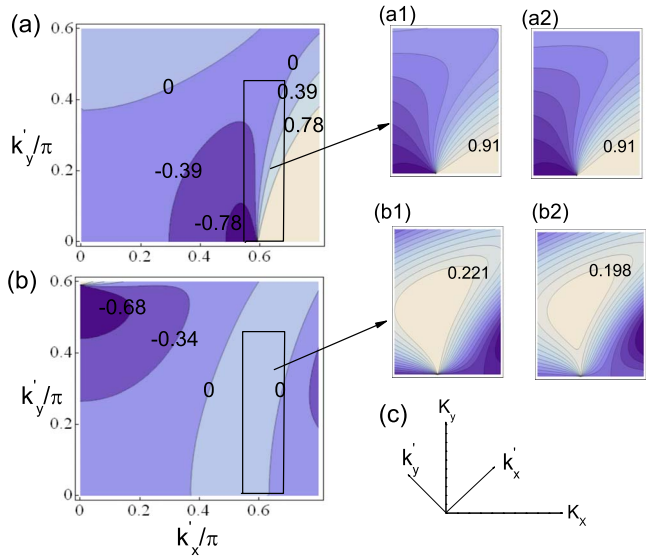


FIG. 4. (Color online) Contour plot of SC quasiparticle velocity (a) $v_{k_x'}$ and (b) $v_{k_y'}$ in the coordinate system $(k_x',k_y')$ for the pristine system with hole doping $\delta=0.15$. (a1) and (b1) show the details for a local region indicated by the square shown in Figs. 4(a) and 4(b), respectively. (a2) and (b2) are the corresponding results for the system with impurity concentration $\Gamma_0/\Delta_0=0.04$. Inset (c) shows the two coordinate systems.

Another feature we can see from Fig. 3 is that the length of the nesting wave vectors shows an unnoticeable variation upon the introduction of impurity. As a result, the incommensurability in the bare spin susceptibility Im $\chi_0$ (without RPA correction) will exhibit negligible difference between the pristine and the impurity-doped systems, as shown in

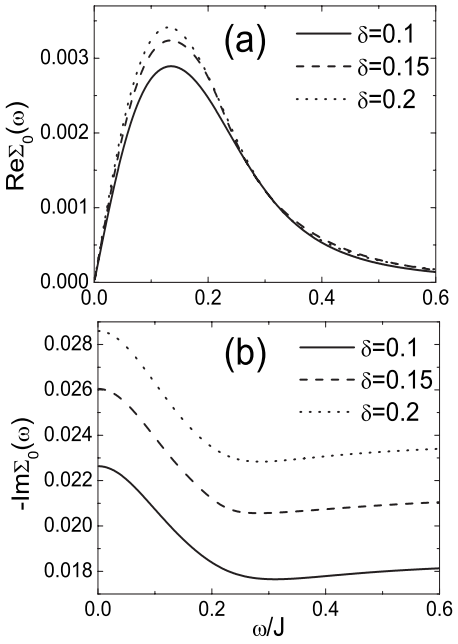


FIG. 5. Real (a) and imaginary parts (b) of the impurity self-energy ($\Sigma_0$) versus $\omega$ at $\Gamma_0/\Delta_0=0.04$ for different hole doping $\delta$. The solid line is for $\delta=0.1$, the dashed line for $\delta=0.15$ and the dotted line for $\delta=0.2$.

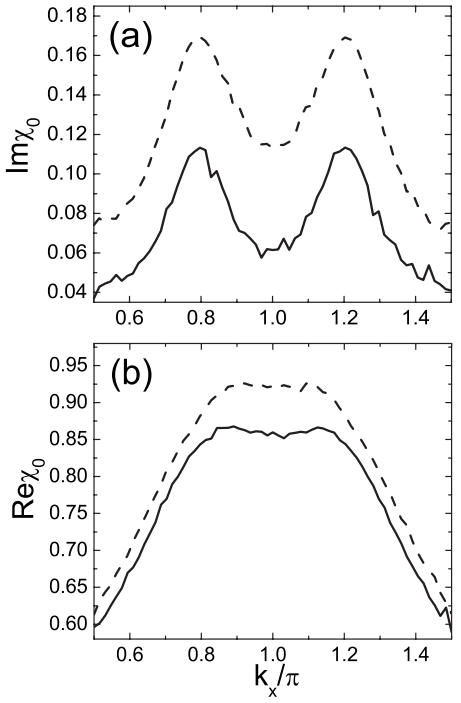


FIG. 6. (a) Imaginary parts and (b) real parts of the bare spin susceptibility $\chi_0$ versus $k_x(k_y=\pi)$ at $\omega=0.2J$, the solid line is for the pristine system and the dashed line for the system with impurity concentration $\Gamma_0/\Delta_0=0.04$. The hole doping $\delta$ is 0.1.

Fig. 6(a). This suggests that the RPA correction plays an important role in the reduction in the incommensurability. When rewriting the renormalized spin susceptibility Eq. (13) via the imaginary part Im $\chi_0$ and the real part Re $\chi_0$ of the bare one, we get Im $\chi$=Im $\chi_0/[(1-U\ \mathrm{Re}\ \chi_0)^2+(U\ \mathrm{Im}\ \chi_0)^2]$. Figure 6(b) shows that Re $\chi_0$ exhibits a flat-top structure around the AF wave vector and its region shrinks upon the introduction of impurity. With the help of the RPA correction factor $(1-U\ \mathrm{Re}\ \chi_0)^2$, this will give rise to the reduction in the incommensurability.

### III. VERTEX CORRECTION

In the above section, we include the multiple noncrossing scattering contributions from impurities through the self-energy correction. Another contribution from impurities is the vertex correction. It accounts for the multiply scattering of the electron and hole excitations in the spin susceptibility off the same impurity. The noncrossing impurity scattering which contributes to the ladder series of diagrams are included by expressing the spin correlation function in terms of a dressed vertex in the SC state,

$$\hat{\chi}_0(\mathbf{q},i\omega_m)=T\sum_n \hat{M}(\mathbf{q},i\omega_m,i\omega_n)\hat{\Lambda}(\mathbf{q},i\omega_m,i\omega_n). \quad (14)$$

Here, $\hat{M}(\mathbf{q},i\omega_m,i\omega_n)$ is a four-component representation of the bubble diagrams, which denotes the bubble diagrams with one particle and one hole line (normal Green's function), one particle and one abnormal Green's function line, one hole and one abnormal Green's function line, and two abnormal Green's function lines, respectively, as shown by Feynman diagrams in Ref. 36. Therefore, Eq. (14) is written as a $4\times4$ matrix. In the case of only the self-energy correction included, the spin susceptibility is represented as a scalar function Eq. (12), because the scattering of electrons and holes off the impurity in the particle-hole excitations is independent, it can be taken into consideration by renormalizing the electron and hole Green's function, respectively.

The dressed vertex is given by the sum of a series of ladder diagrams,

$$\hat{\Lambda}(\mathbf{q},i\omega_m,i\omega_n)=1+\Gamma(i\omega_m,i\omega_n)\hat{M}(\mathbf{q},i\omega_m,i\omega_n)\hat{\Lambda}(\mathbf{q},i\omega_m,i\omega_n), \quad (15)$$

with $\Gamma(i\omega_m,i\omega_n)$ the impurity-scattering line.

The above two equations will yield,

$$\hat{\chi}_0(\mathbf{q},i\omega_m)=T\sum_n \frac{\hat{M}(\mathbf{q},i\omega_m,i\omega_n)}{1-\Gamma(i\omega_m,i\omega_n)\hat{M}(\mathbf{q},i\omega_m,i\omega_n)}. \quad (16)$$

Under the unitary limit, the impurity-scattering lines are given by

$$\Gamma(i\omega_m,i\omega_n)=-\frac{n_i}{(\pi N_0)^2}T_0(i\omega_m,i\omega_n)T_0(i\omega_n). \quad (17)$$

Because the neutron scattering probes the spin-flip particle-hole excitations, the components of $\hat{M}$ that we have to consider should begin and end with opposite spin electron lines.[10,36] Hence, the $4\times4$ spin susceptibility involved here becomes $1\times1$ and is give by,

$$\chi_0=\chi_0^{11}+\chi_0^{14}, \quad (18)$$

with

$$M^{11}(\mathbf{q},i\omega_m,i\omega_n)=-\sum_p G(\mathbf{p}+\mathbf{q},i\omega_m+i\omega_n)G(\mathbf{p},i\omega_n), \quad (19)$$

$$M^{14}(\mathbf{q},i\omega_m,i\omega_n)=-\sum_p F(\mathbf{p}+\mathbf{q},i\omega_m+i\omega_n)F(\mathbf{p},i\omega_n), \quad (20)$$

$G(\mathbf{p},i\omega_n)(F(\mathbf{p},i\omega_n))$ is $G_{11}(G_{12})$ in Eq. (5), representing the normal (abnormal) Green's function with impurity self-energy correction. If summing over one of the Matsubara frequencies in Eqs. (19) and (20), one will find that they are right the two terms of the spin susceptibility with the self-energy correction as given in Eq. (12).

We present Im $\chi$ versus $k_x$ at $\omega=0.02J$ (below the spin gap) and $\omega=0.2J$ (above the spin gap) for two hole dopings in Fig. 7. For a comparison, the result with only impurity self-energy correction is also shown as the dashed-dotted line. For low frequency $\omega=0.02J$, the impurity self-energy correction enhances the intensity of Im $\chi$ noticeably, but it causes no reduction in the incommensurability. The latter feature is different from that obtained at a higher frequency above the spin gap, which shows a reduction in the incommensurability, as shown in Fig. 1 for impurity concentration $\Gamma_0/\Delta_0=0.04$ and in Figs. 7(a′) and 7(b′) for $\Gamma_0/\Delta_0=0.08$.

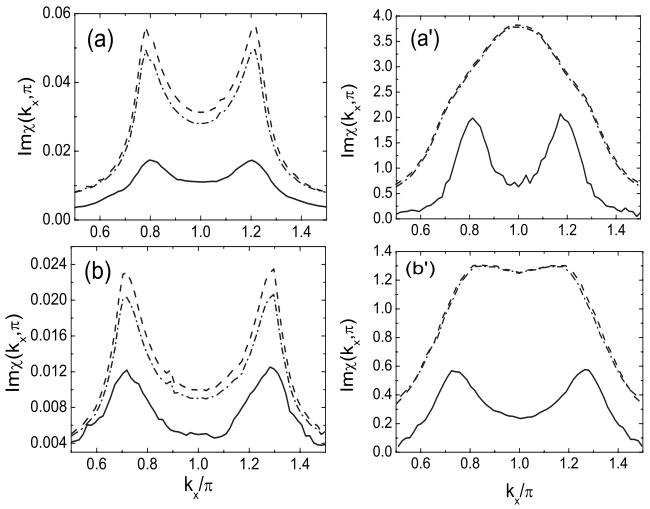


FIG. 7. Im $\chi$ versus $k_x(k_y=\pi)$ at $\omega=0.02J$ below the spin gap [(a) and (b)], and at $\omega=0.2J$ above the spin gap [(a′) and (b′)]. Here, (a) and (a′) are for the hole doping $\delta=0.1$, and (b) and (b′) for $\delta=0.15$. The solid line is for the pristine system and the dashed line for the impurity concentration $\Gamma_0/\Delta_0=0.08$ with vertex correction and the dash-dotted line for that with only the self-energy correction.

Another feature is that the incommensurate structure in the spin response becomes weak gradually with the increase in impurity concentration, and this trend becomes more quick as the hole doping is decreased. One can find that the incommensurate structure is smeared out for $\Gamma_0/\Delta_0=0.08$ and $\delta=0.1$ as shown in Fig. 7(a′). The inclusion of the vertex correction does not change the lineshape qualitatively. In particular, the incommensurability is not altered. In fact, a systematic effect of the vertex correction is to enhance further the intensity of Im $\chi$ inside the spin gap in the momentum region from the incommensurate peak to $(\pi,\pi)$ and this effect do not vary obviously with hole dopings. To look into in detail the effect of the vertex correction, we show the frequency dependence of Im $\chi$ at the IC-peak $Q_\lambda=(0.7\pi,\pi)$ in Fig. 8. One can see that an additional low-energy excitation around $0.04J$ is induced by the vertex correction. It is understood to arise from the multiple scatterings of the particles and holes in spin excitations off the same impurity in the ladder series of diagrams, which gives the vertex correction $\hat{\Lambda}(\mathbf{q},i\omega_m,i\omega_n)=1/[1-\Gamma(i\omega_m,i\omega_n)\hat{M}(\mathbf{q},i\omega_m,i\omega_n)]$ as shown in Eq. (16). Because the impurity self-energy $-\mathrm{Im}\,\Sigma_0$ shows a rapid increase at low frequencies as can be seen in Fig. 5 and correspondingly the impurity-scattering term $\Gamma(i\omega_m,i\omega_n)$ [see Eq. (17)] is increased. This effect will be enhanced largely via the multiple scattering in the form of the vertex correction and lead to the appearance of the low-energy excitation. We notice that a similar emergence of low-energy excitations with Zn doping has been observed by neutron scattering.[25]

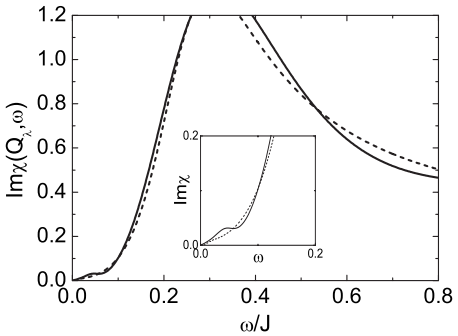


FIG. 8. Im $\chi$ versus $\omega$ at the incommensurate peak $Q_\lambda=(0.7\pi,\pi)$. The solid line is the result with the vertex correction and the dashed line is that without the vertex correction. The hole doping $\delta$ is 0.15 and the impurity concentration $\Gamma_0/\Delta_0=0.08$. The inset shows the fine structure of the low-energy part.

## IV. CONCLUSION

We have studied the nonmagnetic impurity effects on spin excitations in a $d_{x^2-y^2}$-wave superconductor based on the self-consistent $t$-matrix approximation and the weak-coupling RPA-typed approach. The impurity effects are considered based on both the self-energy correction and the vertex correction. Our results show that the self-energy correction will enhance the intensity of spin responses and reduce the incommensurability. These effects are less prominent with the increase in dopings. In the low-energy region inside the spin gap, the intensity in Im $\chi$ is also enhanced, but with no reduction in the incommensurability. The vertex corrections within the ladder approximation do not significantly modify the renormalized-bubble result, but it induces additional excitations in the spin gap. These results are qualitatively consistent with experiments and indicate that the impurity effect on spin response can be consistently accounted for by the weak-coupling RPA-typed approach.

## ACKNOWLEDGMENTS

We thank H. M. Jiang and T. Zhou for useful discussions. This work was supported by the National Natural Science Foundation of China (Grant No. 10525415) and the Ministry of Science and Technology of China (973 project Grants No. 2006CB601002 and No. 2006CB921800).

[1] For reviews, see, R. J. Birgeneau, C. Stock, J. M. Tranquada, and K. Yamada, J. Phys. Soc. Jpn. **75**, 111003 (2006); Y. Sidis, S. Pailhès, B. Keimer, P. Bourges, C. Ulrich, and L. P. Regnault, Phys. Status Solidi **241**, 1204 (2004)

[2] K. Yamada, C. H. Lee, K. Kurahashi, J. Wada, S. Wakimoto, S. Ueki, H. Kimura, Y. Endoh, S. Hosoya, G. Shirane, R. J. Birgeneau, M. Greven, M. A. Kastner, and Y. J. Kim, Phys. Rev. B **57**, 6165 (1998).

[3] P. Dai, H. A. Mook, R. D. Hunt, and F. Dogăn, Phys. Rev. B **63**, 054525 (2001).
[4] M. Fujita, H. Goka, K. Yamada, J. M. Tranquada, and L. P. Regnault, Phys. Rev. B **70**, 104517 (2004).
[5] H. F. Fong, B. Keimer, P. W. Anderson, D. Reznik, F. Doğan, and I. A. Aksay, Phys. Rev. Lett. **75**, 316 (1995).
[6] P. Bourges, Y. Sidis, H. F. Fong, L. P. Regnault, J. Bossy, A. Ivanov, and B. Keimer, Science **288**, 1234 (2000).
[7] J. M. Tranquada, H. Woo, T. G. Perring, H. Goka, G. D. Gu, G. Xu, M. Fujita, and K. Yamada, Nature (London) **429**, 534 (2004).
[8] S. M. Hayden, H. A. Mook, P. C. Dai, T. G. Perring, and F. Doğan, Nature (London) **429**, 531 (2004).
[9] D. Z. Liu, Y. Zha, and K. Levin, Phys. Rev. Lett. **75**, 4130 (1995); N. Bulut and D. J. Scalapino, Phys. Rev. B **53**, 5149 (1996); D. Manske, I. Eremin, and K. H. Bennemann, *ibid.* **63**, 054517 (2001); A. V. Chubukov, B. Janko, and O. Tchernyshyov, *ibid.* **63**, 180507 (2001).
[10] J. X. Li, W. G. Yin, and C. D. Gong, Phys. Rev. B **58**, 2895 (1998).
[11] J. Brinckmann and P. A. Lee, Phys. Rev. Lett. **82**, 2915 (1999); J. X. Li and C. D. Gong, Phys. Rev. B **66**, 014506 (2002).
[12] Y. J. Kao, Q. Si, and K. Levin, Phys. Rev. B **61**, R11898 (2000); A. P. Schnyder, A. Bill, C. Mudry, R. Gilardi, H. M. Ronnow, and J. Mesot, *ibid.* **70**, 214511 (2004); M. R. Norman, *ibid.* **75**, 184514 (2007).
[13] For review, see, S. A. Kivelson, I. P. Bindloss, E. Fradkin, V. Oganesyan, J. M. Tranquada, A. Kapitulnik, and C. Howald, Rev. Mod. Phys. **75**, 1201 (2003).
[14] G. Seibold and J. Lorenzana, Phys. Rev. Lett. **94**, 107006 (2005).
[15] B. M. Andersen and P. Hedegård, Phys. Rev. Lett. **95**, 037002 (2005).
[16] For a review, see, Y. Sidis, P. Bourges, B. Keimer, L. P. Regnault, J. Bossy, A. Ivanov, B. Hennion, P. Gautier-Picard, and G. Collin, *Open Problems in Strongly Correlated Electron Systems*, NATO Science Series II: Mathematics, Physics and Chemistry, Vol. 15, edited by J. Bonca, P. Prelovsek, A. Ramsak, and S. Sarkar (Kluwer Academic Publisher, Dordrecht, 2001), p. 59.
[17] H. Harashina, S. Shamoto, T. Kiyokura, M. Sato, K. Kakurai, and G. Shirane, J. Phys. Soc. Jpn. **62**, 4009 (1993).
[18] Y. Sidis, P. Bourges, B. Hennion, L. P. Regnault, R. Villeneuve, G. Collin, and J. F. Marucco, Phys. Rev. B **53**, 6811 (1996).
[19] G. Khaliullin, R. Kilian, S. Krivenko, and P. Fulde, Phys. Rev. B **56**, 11882 (1997); R. Kilian, S. Krivenko, G. Khaliullin, and P. Fulde, *ibid.* **59**, 14432 (1999).
[20] V. B. Zabolotnyy, S. V. Borisenko, A. A. Kordyuk, J. Fink, J. Geck, A. Koitzsch, M. Knupfer, B. Büchner, H. Berger, A. Erb, C. T. Lin, B. Keimer, and R. Follath, Phys. Rev. Lett. **96**, 037003 (2006).
[21] K. Terashima, H. Matsui, D. Hashimoto, T. Sato, T. Takahashi, H. Ding, T. Yamamoto, and K. Kadowaki, Nat. Phys. **2**, 27 (2006); K. Terashima, T. Sato, K. Nakayama, T. Arakane, T. Takahashi, M. Kofu, and K. Hirota, Phys. Rev. B **77**, 092501 (2008).
[22] T. Sato, K. Terashima, K. Nakayama, S. Souma, T. Takahashi, T. Yamamoto, and K. Kadowaki, Phys. Rev. B **78**, 100502(R) (2008).
[23] M. Kirćan and M. Vojta, Phys. Rev. B **73**, 014516 (2006).
[24] S. Wakimoto, R. J. Birgeneau, A. Kagedan, Hyunkyung Kim, I. Swainson, K. Yamada, and H. Zhang, Phys. Rev. B **72**, 064521 (2005).
[25] M. Kofu, H. Kimura, and K. Hirota, Phys. Rev. B **72**, 064502 (2005).
[26] M. U. Ubbens and P. A. Lee, Phys. Rev. B **46**, 8434 (1992).
[27] P. J. Hirschfeld, P. Wölfle, and D. Einzel, Phys. Rev. B **37**, 83 (1988).
[28] P. J. Hirschfeld and N. Goldenfeld, Phys. Rev. B **48**, 4219 (1993).
[29] S. Schmitt-Rink, K. Miyake, and C. M. Varma, Phys. Rev. Lett. **57**, 2575 (1986).
[30] For a review, see, A. V. Balatsky, I. Vekhter, and J.-X. Zhu, Rev. Mod. Phys. **78**, 373 (2006).
[31] Y. Sun and K. Maki, Phys. Rev. B **51**, 6059 (1995).
[32] A. A. Abrikosov and L. P. Gor'kov, Zh. Eksp. Teor. Fiz. **39**, 1781 (1960) [Sov. Phys. JETP **12**, 1243 (1961)].
[33] R. J. Radtke, K. Levin, H. B. Schüttler, and M. R. Norman, Phys. Rev. B **48**, 653 (1993).
[34] H. J. Vidberg and J. W. Serene, J. Low Temp. Phys. **29**, 179 (1977).
[35] D. C. Zhang and J. X. Li, Phys. Rev. B **79**, 064512 (2009).
[36] S. M. Quinlan and D. J. Scalapino, Phys. Rev. B **51**, 497 (1995).